CHEMISTRY OF MATERIALS
Article

Chem. Mater. **2010,** *22,* 4263–4270 4263
DOI:10.1021/cm101240n

Molecular Precursor Route to a Metastable Form of Zinc Oxide

Carlos Lizandara Pueyo,[†] Stephan Siroky,[†] Steve Landsmann,[†] Maurits W. E. van den Berg,[‡] Markus R. Wagner,[§] Juan S. Reparaz,[§] Axel Hoffmann,[§] and Sebastian Polarz*[,†]

[†]*Department for Chemistry, University of Konstanz, D-78457 Konstanz, Germany,* [‡]*Tronox Pigments GmbH, Rheinuferstrasse 7-9, D-47829 Krefeld, Germany, and* [§]*Institute for Solid-State Physics, Technical University Berlin, Hardenbergstrasse 36, 10623 Berlin, Germany*

Received May 3, 2010. Revised Manuscript Received June 9, 2010

Important changes in properties are observed in many instances when, at constant composition, materials possessing different crystal structure, so-called polymorphs are considered. Because many viable polymorphs have not yet been realized experimentally, it is an important task to learn about the factors which determine the formation of metastable phases. The preparation of such phases is particularly challenging when the thermodynamically stable phase forms already under mild conditions. Zinc oxide with Wurtzite structure represents such a case, and because of its multifunctional character, it is currently in the focus of research in many areas. Thus, it can be envisioned that zinc oxide materials with a structure different to Wurtzite will exhibit new, exciting, and eventually unforeseeable properties. The preparation of ZnO under kinetically controlled conditions using an organometallic precursor system is presented here. The formation of a new, nanocrystalline phase with 99% purity has been observed at low temperatures (T = 2 °C). The analysis of the new phase with a variety of analytical methods including powder X-ray diffraction (PXRD), differential scanning calorimetry (DSC), X-ray absorption near-edge spectra (XANES)/extended X-ray absorption fine structure (EXAFS), high-resolution transmission electron microscopy (HRTEM), FT-Raman and optical spectroscopy leads to the conclusion that a metastable ZnO with a crystal structure resembling the α-boron nitride structure has been prepared. The formation of this material represents a novel example for the application of the Ostwald step-rule in materials science.

Introduction

Materials scientists have successfully explored various possibilities to tune the properties of materials. It is taken for granted that the synthesis of solids with new composition will always take a prominent place in the quest for materials for future applications. It is less obvious that significant changes in properties are observed in many instances, when, at constant composition, material parameters like particle size, surface structure, particle shape, and so forth are modified. An excellent example is the so-called quantum-size effect. The energy gap between the valence band and the conduction band changes significantly if the size of a particle is confined in all three dimensions typically below 10 nm.[1]

It is important to note that also crystal structure is crucial. The extent of deviation in properties depends the coordination shell in which the differences in crystal structure occur. Maximal differences in physical and chemical properties are caused by a change in the first coordination shell, as in the case of Graphite (coordination number N_c = 3) and Diamond (N_c = 4). Graphite is a mechanically relatively soft material, a two-dimensional conductor with black color while diamond is an insulating and transparent material with great hardness. More subtle but nevertheless important differences are observed if higher coordination shells are affected. A case in point are the changes in photocatalytic activity found for different modifications of titania.[2]

Surprisingly, only a minority of viable polymorphs have already been "manufactured".[3] Thus, the exploration of routes leading to new polymorphs is auspicious and important, but it is also extremely difficult. It is hard to identify only one particular reason why the synthesis of metastable polymorphs is so demanding. The metastable modifications can be described as local minima on a multidimensional energy hypersurface. Jansen has pioneered in several inspiring papers the concept of the so-called energy landscapes.[4,5] Although it is possible in the meantime to estimate the viability of a certain structure using advanced computational methods, because of the complexity of the

*To whom correspondence should be addressed. E-mail: sebastian.polarz@uni-konstanz.de.

(1) (a) Weller, H. *Adv. Mater.* **1993**, *5*, 88. (b) Weller, H. *Angew. Chem., Int. Ed. Engl.* **1993**, *32*, 41.

(2) (a) Carp, O.; Huisman, C. L.; Reller, A. *Prog. Solid State Chem.* **2004**, *32*, 33. (b) Glassford, K. M.; Chelikowsky, J. R. *Phys. Rev. B* **1992**, *46*, 1284. (c) Mo, S. D.; Ching, W. Y. *Phys. Rev. B* **1995**, *51*, 13023.

(3) (a) van den Streek, J. *Acta Crystallogr., Sect. B: Struct. Sci.* **2006**, *62*, 567. (b) Jansen, M.; Schoen, J. *Z. Anorg. Allg. Chem.* **1998**, *624*, 533.

(4) (a) Schoen, J. C.; Jansen, M. *Inorg. Chem. Highlights* **2002**, 55. (b) Schoen, J. C.; Jansen, M. *Z. Kristallogr.* **2001**, *216*, 307. (c) Doll, K.; Schoen, J. C.; Jansen, M. *Phys. Chem. Chem. Phys.* **2007**, *9*, 6128.

(5) Jansen, M. *Angew. Chem., Int. Ed.* **2002**, *41*, 3746.

Published on Web 06/18/2010

systems caused by the large number of parameters and interacting species, it will remain impossible to calculate the successful paths on the energy landscape leading to a desired local minimum.[5] However, there are some general guidelines which are still valid although they have already been developed over 100 years ago. If a reaction can result in several products, it is not the global minimum state with the least amount of free energy that is obtained initially, but the least stable one, lying nearest to the original state in free energy. This statement constitutes Ostwald's step rule on the law of successive reactions.[6] Thus, the resulting guideline can be formulated as follows: The chances for the synthesis of materials with metastable crystal structure can be enhanced if a route can be taken which is strictly kinetically controlled.

Jansen and co-workers could prepare several metastable modifications of binary ionic solids using a low-temperature deposition technique.[7] The salt is evaporated and deposited as a relatively thin film on a cold substrate (e.g., $T = -100$ °C). The following crystallization process obeys the Ostwald's step rule and could be monitored by powder X-ray diffraction (PXRD). The latter experiments show that it is of elemental importance to conduct a process at such low temperatures that the energy barrier leading to the global minimum is not surmounted.

Therefore, it can be expected that it will be very difficult to realize metastable states for solids that are characterized by low crystallization temperatures. One example of particular relevance is zinc oxide (ZnO) in Wurtzite modification.[8] Approximately 2500 papers are currently published per year related to ZnO. This tremendous interest is provoked by the multifunctional character of ZnO: It is a II−VI wide-gap semiconductor with applications in optoelectronics,[9] gas sensing,[10] catalysis, and far more.[11,12] ZnO with a crystal structure different from that of Wurtzite is likely to have new and unforeseeable properties.[13] Metastable ZnO modifications have by now been reported only as "exotic phenomena" and in small amounts: Under high pressure ($p > 8.7$ GPa)[14] and room temperature conditions, a Rock Salt-ZnO was described.[15] Thin Sphalerite-ZnO films were obtained via epitaxial growth.[16] Seshadri and co-workers have reported an innovative approach for the synthesis of Sphalerite-ZnO in 2005.[17] The authors have treated conventional ZnO with 2,4-pentanedione at elevated temperatures, followed by decomposition at 573 K. As a result a composite between Wurtzite-ZnO and Sphalerite-ZnO has been obtained. Several additional polymorphs have been predicted as viable by quantum-chemical methods, for instance, ZnO with α-boron nitride (αBN-ZnO) structure.[18−20] Tusche and co-workers have studied ultrathin ZnO films (2−5 monolayers) on Ag(111) surfaces and have described the formation of αBN-ZnO at the surfaces.[21] Furthermore, an interesting paper has been published by Zhao and co-workers on $(ZnO)_{60}$ clusters.[22] According to their DFT calculations even a zinc oxide material resembling a zeolite structure (sodalite) should be possible.

Metastable polymorphs of ionic solids are have also been found in some biominerals.[23] From biomineralization it is known that information about a metastable crystal phase is already present at the stage of critical nuclei during early crystallization.[24,25] If the critical nuclei exhibit the structure of the thermodynamically stable phase, it will be impossible to obtain the metastable material later on. Since the critical nuclei are small (<2 nm) and form early in the reaction under non-equilibrium conditions, insufficient knowledge is available concerning the processes and factors which determine the structure of the solid material formed during the transition from a supersaturated state and the restructuring processes during growth. Recently, Coelfen and co-workers argued that so-called pre-nucleation clusters are deciding in the structure formation of biomimetic $CaCO_3$.[25]

The idea to prepare materials with metastable crystal structure at mild conditions at a state close to the critical nucleus for instance by starting from molecular clusters resembling the topology of the desired phase is very appealing. However, yet there are only few examples for such a "*Topological Synthesis*". An impressive example has been reported by Barron and co-workers.[26] When the

(6) Ostwald, W. *Z. Phys. Chem.* **1879**, *22*, 289.
(7) (a) Fischer, D.; Jansen, M. *J. Am. Chem. Soc.* **2002**, *124*, 3488. (b) Fischer, D.; Jansen, M. *Angew. Chem., Int. Ed.* **2002**, *41*, 1755. (c) Liebold-Ribeiro, Y.; Fischer, D.; Jansen, M. *Angew. Chem., Int. Ed.* **2008**, *47*, 4428.
(8) Liu, B.; Zeng, H. C. *Langmuir* **2004**, *20*, 4196.
(9) (a) Look, D. C.; Claftin, B. *Phys. Status Solidi B* **2004**, *241*, 624. (b) Meyer, B. K.; Alves, H.; Hofmann, D. M.; Kriegseis, W.; Forster, D.; Bertram, F.; Christen, J.; Hoffmann, A.; Strassburg, M.; Dworzak, M.; Haboeck, U.; Rodina, A. V. *Phys. Status Solidi B* **2004**, *241*, 231. (c) Monroy, E.; Omnes, F.; Calle, F. *Semicond. Sci. Technol.* **2003**, *18*, R33.
(10) Polarz, S.; Roy, A.; Lehmann, M.; Driess, M.; Kruis, F. E.; Hoffmann, A.; Zimmer, P. *Adv. Funct. Mater.* **2007**, *17*, 1385.
(11) (a) Peppley, B. A.; Amphlett, J. C.; Kearns, L. M.; Mann, R. F. *Appl. Catal., A* **1999**, *179*, 21. (b) Woell, C. *Prog. Surf. Sci.* **2007**, *82*, 55.
(12) Polarz, S.; Neues, F.; Van den Berg, M.; Grünert, W.; Khodeir, L. *J. Am. Chem. Soc.* **2005**, *127*, 12028.
(13) (a) Murayama, M.; Nakayama, T. *Phys. Rev. B* **1994**, *49*, 4710. (b) Zhang, L. X.; Huang, H. C. *Appl. Phys. Lett.* **2007**, *90*, 023115. (c) Ashrafi, A.; Jagadish, C. *J. Appl. Phys.* **2007**, *102*, 071101.
(14) Decremps, F.; Zhang, J.; Liebermann, R. C. *Europhys. Lett.* **2000**, *51*, 268.
(15) (a) Gerward, L.; Olsen, J. S. *J. Synchrotron Radiat.* **1995**, *2*, 233. (b) Cai, J.; Chen, N. X. *J. Phys.: Condens. Matter* **2007**, 19.
(16) (a) Ashrafi, A.; Ueta, A.; Avramescu, A.; Kumano, H.; Suemune, I.; Ok, Y. W.; Seong, T. Y. *Appl. Phys. Lett.* **2000**, *76*, 550. (b) Lee, G. H.; Kawazoe, T.; Ohtsu, M. *Appl. Surf. Sci.* **2005**, *239*, 394.
(17) Snedeker, L. P.; Risbud, A. S.; Masala, M.; Zhang, J. P.; Seshadri, R. *Solid State Sci.* **2005**, *7*, 1500.
(18) (a) Freeman, C. L.; Claeyssens, F.; Allan, N. L.; Harding, J. H. *Phys. Rev. Lett.* **2006**, *96*, 066102. (b) Wen, B.; Melnik, R. *Chem. Phys. Lett.* **2008**, *466*, 84.
(19) Coasne, B.; Mezy, A.; Pellenq, R. J. M.; Ravot, D.; Tedenac, J. C. *J. Am. Chem. Soc.* **2009**, *131*, 2185.
(20) Schoen, J. C.; Jansen, M. *Angew. Chem., Int. Ed. Engl.* **1996**, *35*, 1287.
(21) Tusche, C.; Meyerheim, H. L.; Kirschner, J. *Phys. Rev. Lett.* **2007**, 99.
(22) Wang, B.; Wang, X.; Zhao, J. *J. Phys. Chem. C* **2010**, *114*, 5741.
(23) (a) Volkmer, D. *Initiativen zum Umweltschutz* **2002**, *41*, 107. Lowenstam, H. A.; Weiner, S. *On Biomineralization*; Oxford University Press: New York, 1989.
(24) Mann, S.; Ozin, G. A. *Nature* **1996**, *382*, 313.
(25) Gebauer, D.; Voelkel, A.; Coelfen, H. *Science* **2008**, *322*, 1819.
(26) (a) Macinnes, A. N.; Power, M. B.; Barron, A. R.; Jenkins, P. P.; Hepp, A. F. *Appl. Phys. Lett.* **1993**, *62*, 711. (b) Macinnes, A. N.; Power, M. B.; Barron, A. R. *Chem. Mater.* **1993**, *5*, 1. (c) Macinnes, A. N.; Power, M. B.; Barron, A. R. *Chem. Mater.* **1992**, *4*, 11.

Scheme 1. Schematical Representation of the "Topological Synthesis" Concept Indicated for Binary Solids[a]

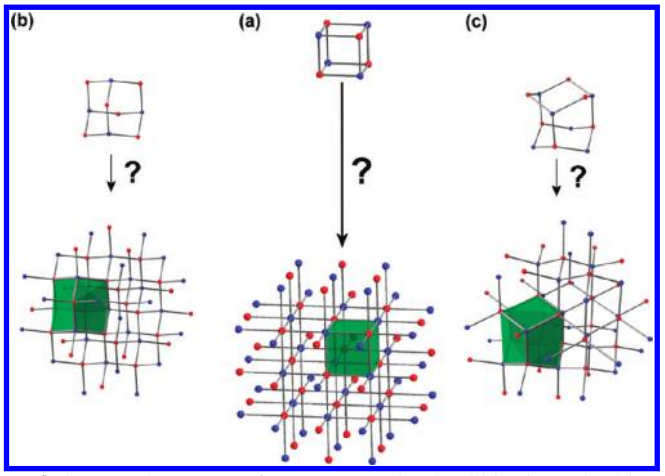

[a] The crystal structure of a target material should be determined by the topology of a molecular precursor comprising a "M_xE_y" cluster core (M ≡ metal atom; E ≡ O, S, ...). Target materials with Rock Salt structure (a), Sphalerite structure (b), and Wurtzite structure (c) are highlighted.

Scheme 2. Qualitative Potential Energy Diagram for the Formation of the Different ZnO Materials Starting from Organometallic $[MeZnO^{tert}Bu]_4$ Heterocubanes As Precursors (a), the Proposed Structure for the Instable Intermediate (b), the Resulting Metastable ZnO with α-BN Structure (c), and the Thermodynamically Stable Wurtzite-ZnO (d)

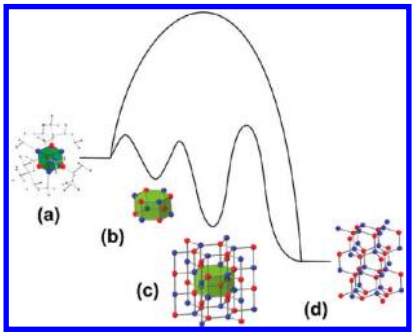

authors used the dimeric $[(^tBu)_2GaS^tBu]_2$ as a precursor for the synthesis of GaS they obtained the thermodynamically most stable hexagonal modification. However, when $[Ga(^tBu)S]_4$ with heterocubane topology was used GaS with cubic symmetry could be prepared. Barron et co-workers have reported a similar approach leading to metastable InS and GaS.[27] The "Topological Synthesis" concept is indicated in Scheme 1. It can be envisioned that the condensation of oxo-clusters with heterocubane topology could ultimately lead to the formation of materials with Rock Salt structure. In addition, it could be possible to produce metastable materials with Zinc Blende structure by using precursors with adamantane topology (see Scheme 1b), or metastable Wurtzite materials from the respective molecular cluster compound shown in Scheme 1c. The latter two approaches could be very interesting for solids for which the most stable modification possesses cubic symmetry (e.g., MgO, NiO, MnS, ZrO_2, CeO_2, RhO_2, Mn_2O_3, FeS_2, $CaTiO_3$, $SrFeO_3$, ReO_3, WO_3, etc.).[28]

Our group has been concerned with the preparation of various ZnO materials using organometallic precursor compounds comprising a "Zn_4O_4" heterocubane entity (see also Scheme 2a).[12,29] We have recently used this precursor system for a detailed in situ study of the low-temperature nucleation and growth of ZnO in organic solvents (e.g., thf, pentane, etc.).[30] The advantage of using organic solvents is that because of the low solubility of ions in the continuous phase secondary, equilibrating processes like Ostwald ripening are effectively suppressed. Motivated by the work by Barron and co-workers and based on the profound experience with $[MeZnOR]_4$ heterocubanes,[30] here, we report about the synthesis of ZnO under kinetically controlled conditions using the mentioned organometallic precursors.

Results and Discussion

Like expected and described previously,[30] under conditions of slow nucleation and growth only the formation of the Wurtzite modification could be observed. However, assuming that an alternative product might be obtained under kinetically controlled conditions the rate of the reaction v (see eq 1) was increased by working at much higher concentrations of the reactants.

$$v_{X-phase/W-ZnO} = \frac{dc_{ZnO}(t)}{dt} = k_{X-phase/W-ZnO}(T)\cdot c_{[MeZnOR]_4}(t)^{n1}\cdot C_{H_2O}(t)^{n2} \quad (1)$$

with $v \cong$ the reaction rate, $t \cong$ time, $k \cong$ the reaction rate constant, $n \cong$ the reaction order.

Eventually, the emergence of an impurity has been observed by PXRD shown in Figure 1a. The comparison of these reflexes with databases like ICDD did not reveal any coincidence with previously reported materials, in particular not with zinc-oxo-hydroxo phases (ZnO_{1-x}-$(OH)_y$) which might be expected to form as a side product. The observed reflexes are assigned to a new material, denoted as "X-phase". Unfortunately, for the phase mixture shown in Figure 1a it is impossible to obtain reliable information about the structure of the new material. The attempt to increase the amount of the X-phase by making the reaction even faster (by increasing the reactant concentration further) failed because of the quick precipitation of the product in the used organic solvent (tetrahydrofuran). The early precipitation resulting in a shortened growth period can possibly be avoided by using a suitable agent for the colloidal stabilization of the evolving inorganic

(27) (a) Maclnnes, A. N.; Cleaver, W. M.; Barron, A. R.; Power, M. B.; Hepp, A. F. *Adv. Mater. Opt. Electron.* **1992**, *1*, 229. (b) Keys, A.; Bott, S. G.; Barron, A. R. *Chem. Mater.* **1999**, *11*, 3578–3587.

(28) Isobe, K.; Yagasaki, A. *Acc. Chem. Res.* **1993**, *26*, 524.

(29) (a) Polarz, S.; Strunk, J.; Ischenko, V.; Van den Berg, M.; Hinrichsen, O.; Muhler, M.; Driess, M. *Angew. Chem.* **2006**, *118*, 3031; (b) Polarz, S.; Roy, A.; Merz, M.; Halm, S.; Schröder, D.; Scheider, L.; Bacher, G.; Kruis, F. E.; Driess, M. *Small* **2005**, *1*, 540. (c) Polarz, S.; Orlov, A.; Van den Berg, M.; Driess, M. *Angew. Chem., Int. Ed.* **2005**, *44*, 7892. (d) Ischenko, V.; Polarz, S.; Grote, D.; Stavarache, V.; Fink, K.; Driess, M. *Adv. Funct. Mater.* **2005**, *15*, 1945.

(30) Lizandara-Pueyo, C.; van den Berg, M.; de Toni, A.; Goes, T.; Polarz, S. *J. Am. Chem. Soc.* **2008**, *130*, 16601.

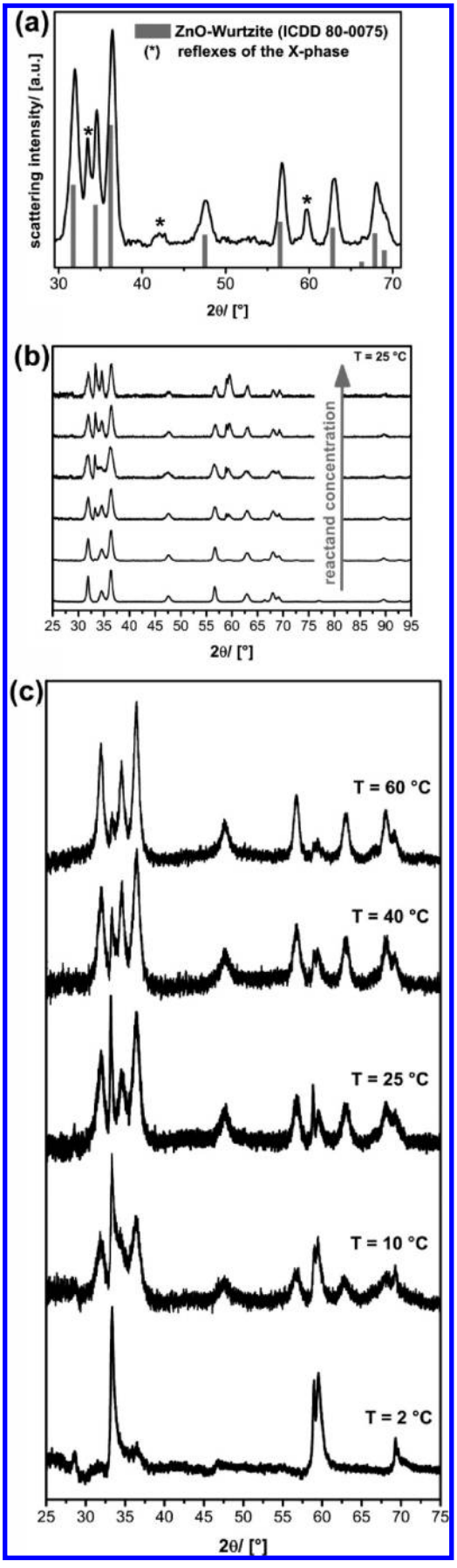

Figure 1. PXRD data of the material obtained by rapid ZnO formation (a),with PVP as a colloidal stabilizer for different reactant concentrations (b), and in dependence of temperature (c).

particles. The polymer poly(vinylpyrrolidone) (PVP) has been described to be very suitable for the colloidal stabilization of zinc oxide by different groups who have also recognized some interesting morphological effects when ZnO was prepared in the presence of PVP.[31] Because of the latter arguments PVP has also been used in the current study. As a result it was possible to increase the reactant concentration further without too early precipitation. Marked effects on the amount of formed X-phase have been observed (see Figure 1b). For instance, an excess of water, which leads to faster ZnO formation, results in increasing proportions of the "X-phase" of up to 50%.

On the other hand, the influence of the temperature was quite unexpected. Accelerating the process further via an increase of temperature (25 °C → 40 °C → 60 °C → 80 °C) causes the X-phase to vanish more and more, while a decrease of the temperature has the opposite effect (Figure 1c). At $T = 2$ °C a material can be obtained which contains 99% of the X-phase and only 1% Wurtzite-ZnO (W-ZnO). The effects of reactant concentration and of process temperature can be understood if one assumes that the transformation of the precursor to one or the other of the alternative products (X-phase or W-ZnO) is associated with different activation energies E_a, of which that for the formation of the "X-phase" is lower than that for formation of W-ZnO ($\Rightarrow k_{X\text{-}phase} > k_{W\text{-}ZnO}$; eq 1 and Scheme 2). Interestingly, the reflexes of the X-phase are narrower than those belonging to W-ZnO (Figure 1). This indicates the formation of larger particles of the X-phase. The latter observation is consistent with the assumption that the rate of formation of the X-phase is higher. Under rapid nucleation and growth conditions (high reactant concentrations) the pathway leading to the "X-phase" can be populated to a certain degree because it is associated with the larger rate, but only as long as the thermal energy is not sufficient to surmount the energy barrier leading to W-ZnO (see Scheme 2). It seems that the X-phase is the kinetic product.

As the unknown material can now be prepared in almost pure form it is possible to study its properties in more detail. The stability of the "X-phase" was investigated by temperature-dependent in situ PXRD (shown in Figure 2a) and differential scanning calorimetry (DSC) measurements. The reflexes of the "X-phase" vanish at temperatures $T > 200$ °C and the pattern typical for W-ZnO appears (Figure 2a). An alternative representation of the PXRD data is also shown in the Supporting Information, Figure SI-1. DSC data indicate an irreversible phase transition in the temperature interval 220−280 °C, in agreement with the PXRD data (Supporting Information, Figure SI-1). Because the "X-phase" transforms directly into W-ZnO (for a graphical representation

(31) (a) Zhang, J. H.; Liu, H. Y.; Wang, Z. L.; Ming, N. B.; Li, Z. R.; Biris, A. S. *Adv. Funct. Mater.* **2007**, *17*, 3897. (b) Biswas, K.; Das, B.; Rao, C. N. R. *J. Phys. Chem. C* **2008**, *112*, 2404. (c) Lipowsky, P.; Hedin, N.; Bill, J.; Hoffmann, L. C.; Ahniyaz, A.; Aldinger, F.; Bergstrom, L. *J. Phys. Chem. C* **2008**, *112*, 5373. (d) Wei, S. F.; Lian, J. S.; Jiang, Q. *Appl. Surf. Sci.* **2009**, *255*, 6978.

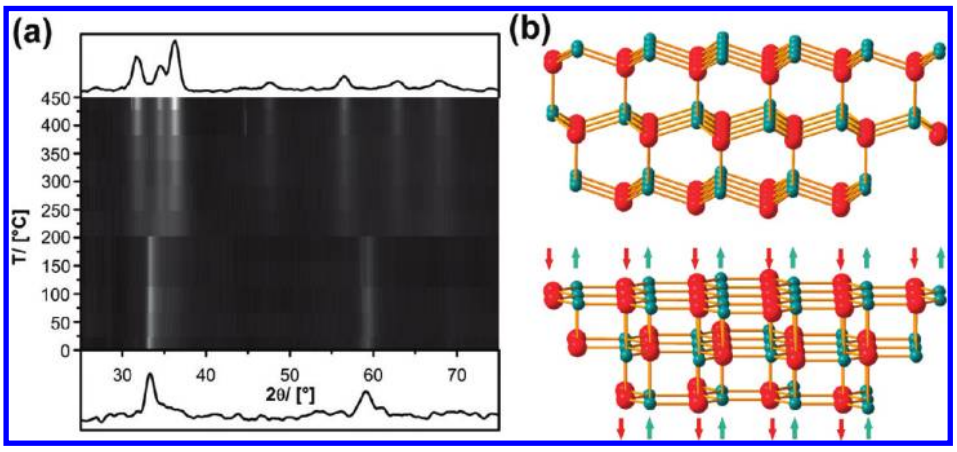

Figure 2. (a) Temperature-dependent in situ investigation of the transformation of the "X-phase" into Wurtzite by PXRD. The intensity of the reflexes is encoded as brightness values. The diffraction patterns for the initial state (at $T = 20$ °C; "X-phase") and the product (at $T = 500$ °C, Wurtzite) are plotted as a conventional x, y plot. An alternative plot of the data is shown in Supporting Information, Figure SI-1. (b) The transformation of the α-BN lattice into the Wurtzite lattice. The arrows indicate the direction in which oxygen and zinc atoms move.

see also Figure 2b) one might suppose that it is a new, metastable form of ZnO.

However, at the present moment this is not more than a hypothesis. The first alternative possibility is that the X-phase might be a composite arising as a product of the direct reaction of PVP with the precursor $[MeZnOR]_4$ (and water). Here, it is important to note that a mixture of the X-phase and W-ZnO could also be obtained without the use of any additive (see above; Figure 1a). Furthermore, alternative agents for the colloidal stabilization can also be applied successfully. Also in these cases it is possible to prepare the pure X-phase. Palmitic acid is shown as a representative case in the Supporting Information, Figure SI-2. The experiments described above prove unequivocally that the occurrence of the X-phase is not causally related to the presence of PVP or any other additive! The next, yet remaining possibility is that the X-phase is not pure inorganic in nature but represents a partially reacted, intermediary organometallic zinc-oxo-(hydroxo) precursor phase, $Me_wZnO_x(^{tert}Bu)_y(OH)_z$. The latter question is extremely difficult to clarify. It has already been mentioned that PVP fulfills an important function: It keeps the growing particles in the homogeneous phase during growth. Therefore, PVP is bound to the surfaces of the particles, and its complete removal is not possible. The amount of inorganic material can be as high as ≈70% depending on synthesis conditions. However, this also means that the analytical trace of PVP is observed together with the X-phase in many analytical techniques (see also Supporting Information, Figure SI-3). The FT-IR spectrum of the prepared material contains solely bands characteristic for PVP and no bands originating from additional organic groups are seen. Thus, it can be excluded that there are no residual organic groups (except for PVP) present in the X-phase. The latter conclusion is supported by elemental analysis. Furthermore, provided that PVP is not the only carbon-containing component in the obtained material one expects that the ratio of nitrogen to carbon is lower in comparison to pure PVP (N/C = 19.7%) as a reference. The N/C ratio in the product (PVP/X-phase) is 19.6%.

The X-phase is purely inorganic in nature. Thus, the hypothesis that the X-phase is a metastable modification of ZnO becomes more likely, and we come back to the evaluation of its structure. Considering the rare reports about the experimental realizations of metastable ZnO phases in the literature two eligible proposals are the Rock Salt-ZnO (RS-ZnO) or the Zinc Blende-ZnO (ZB-ZnO).[15−17] However, the PXRD pattern is neither consistent with the cubic forms RS-ZnO or ZB-ZnO. The lattice of the X-phase clearly possesses hexagonal symmetry. The latter condition is fulfilled for ZnO with α-boron nitride structure (αBN-ZnO) predicted theoretically, but not realized experimentally.[18,19]

A full profile analysis of the PXRD data using the Rietveld method shown in Figure 3a was performed presuming a mixture of αBN-ZnO (space group $P6_3/mmc$) and W-ZnO (space group $P6_3mc$). It can be seen that there is an excellent compliance between the Rietveld simulation and the experimental data. The structure of the αBN-ZnO phase is shown in Scheme 2c and Figure 2b, and an alternative representation is given in the Supporting Information, Figure SI-4. The relative amount of the X-phase is 99.2%, and the lattice parameters are a = 3.099 Å and c = 3.858 Å. The αBN-ZnO structure comprises layers of condensed, planar "Zn_3O_3" rings. The Zn−O distance in the layers is 1.791 Å and the layer-to-layer distance is 1.928 Å (d_{002}). The findings are in good agreement to the data by Tusche and co-workers who have studied ultrathin layers of ZnO on silver surfaces (d_{ZnO} = 1.92 Å).[21] The interlayer-distance is clearly too small if only van der Waals interactions between the layers are considered. Thus, Zn^{2+} is coordinated to three oxygen ligands within the layer and to two additional oxygen atoms above and below, resulting in a (5/5)-coordination.

Independent analytical techniques were applied for securing the hypothesis that the X-phase is a metastable ZnO phase with α-BN structure. X-ray absorption Zn−K near-edge spectra XANES, extended X-ray absorption fine structure data (EXAFS; Figure 3b), and high resolution transmission electron microscopy (HRTEM) images

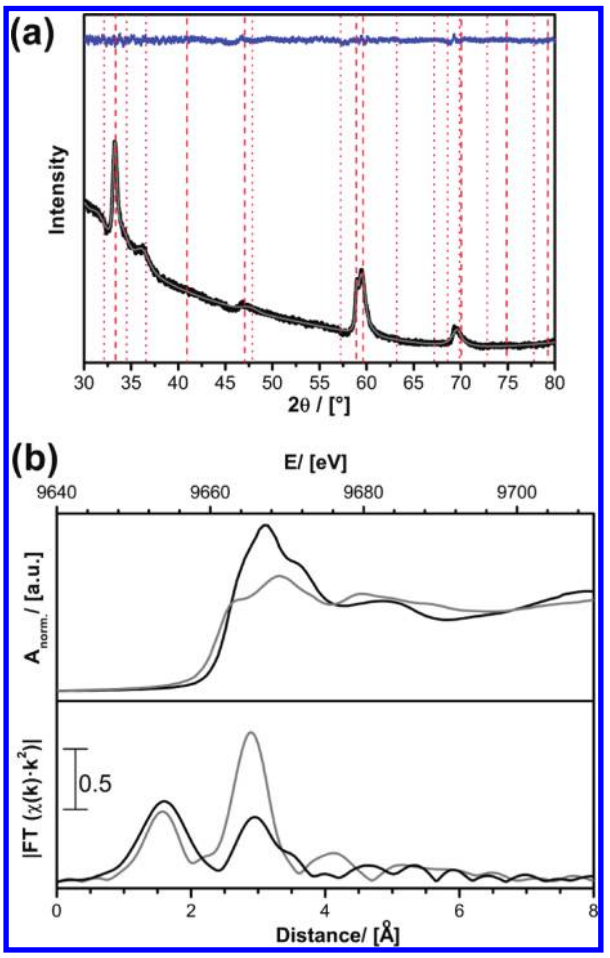

Figure 3. (a) Experimental PXRD pattern of the X-phase (black graph), the Rietveld simulation (gray) of the data considering a mixture of αBN-ZnO (red dashed lines), and W-ZnO (red dotted lines). The difference between the experimental data and the simulation is shown in blue. (b) Zn K-edge XANES (top) and EXAFS (bottom) data are shown for the "X-phase" (black) and for W-ZnO as a reference (gray).

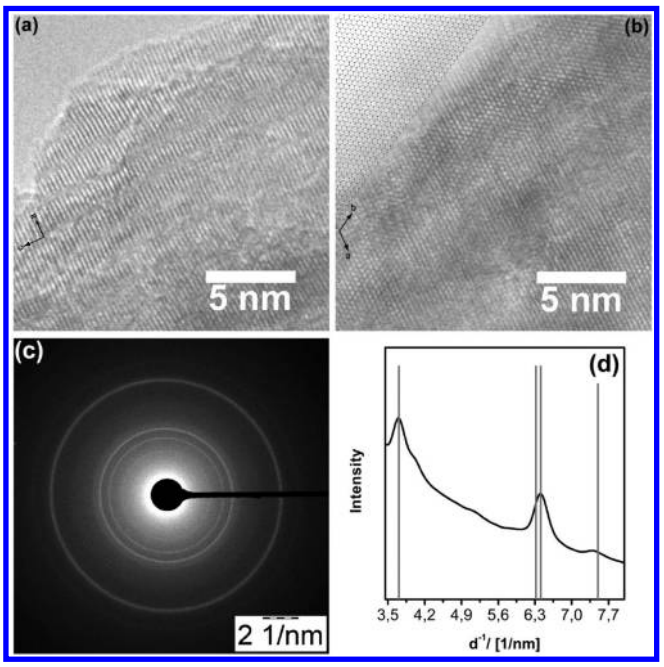

Figure 4. (a, b) HRTEM images of the "X-phase". For better visibility of the agreement between the micrographs and the structure of the (5/5)-ZnO form, an overlay of the latter has been added (upper left corner). (c) Electron diffraction image recorded with conventional TEM. (d) Electron diffraction pattern (black) in comparison to the main diffraction signals from PXRD (gray).

(Figure 4a,b) were acquired. Inspection of the XANES and EXAFS data and comparison to standard ZnO as a reference confirms once more, that the X-phase is not Wurtzite. An adequate simulation of the EXAFS data was possible neither assuming the Wurtzite structure nor a graphitic (3/3)-structure. Only the (5/5)-structure gave satisfactory results (shown in Supporting Information, Figure SI-5). The findings from PXRD, XANES, and EXAFS are supported by the TEM results shown in Figure 4. The HRTEM micrographs exhibit two important features. The undulated lattice fringes seen in Figure 4a ($d \approx 2.0$ Å) fit well to the d_{002} value of the (5/5)-structure, and the image shown in Figure 4b correlates well the characteristic structure of the [001]-layer. Electron diffraction was recorded, using conventional TEM (Figure 4c). Because an area containing several particles of the X-phase was probed, one obtains a set of characteristic diffraction fringes. The radial integration of the electron diffraction pattern is shown as a 2-D graph in Figure 4d. The electron diffraction signals corresponding to $d = 0.270, 0.156, 0.133$ nm fit perfectly to the reflexes observed in PXRD. The weaker reflexes at lower angle are due to PVP (see also Supporting Information, Figure SI-3). Finally, FT-Raman measurements were performed. The α−BN structure has the symmetry group D^4_{6h} ($P6_3/mmc$) with the irreducible representation $\Gamma = 2E_{2g} + A_{2u} + E_{1u} + 2B_{1g}$ of which only the two E_{2g} modes are Raman active (Figure 5a).[16] As the phase transition to the W-ZnO structure with the space group C^4_{6v} ($P6_3mc$) occurs, the irreducible representation is changed so that E_{2g} modes of the X-phase disappear whereas the Raman modes related to the Wurtzite structure become allowed (Figure 5a). In particular, these are the narrow E_2(high) at 438.1 cm^{-1}, the A_1(TO) at 380 cm^{-1}, a weak shoulder in the range of the A_1/E_1(LO) around 578 cm^{-1} as well as several second order modes.[17] Also Raman spectroscopy supports the hypothesis that the X-phase is the metastable (5/5) form of ZnO.

Because of the variation in coordination type, it can also be expected that the (5/5) form of ZnO present in the X-phase will possess different electronic properties than W-ZnO. Band-gap energies of the materials were obtained by measuring diffuse reflectance spectra in the UV−vis region. In Figure 5b the modified Kubelka−Munk function $[F(R_\infty)h\nu]^{1/2}$ is plotted versus the incident photon energy as required for an indirect crystalline semicondutor.[32] In comparison to W-ZnO ($E_{gap} = 3.3$ eV), the energy of the band gap is seen to be significantly larger for the X-phase ($E_{gap} = 3.5$ eV). The results are in agreement with the mentioned theoretical studies on the (5/5)-structure, in which an increase of the band gap has been predicted.[18]

(32) (a) Kubelka, P. *J. Opt. Soc. Am.* **1948**, *38*, 448. (b) Yang, L.; Kruse, B.; Miklavcic, S. J. *J. Opt. Soc. Amq. A* **2004**, *21*, 1942. (c) Yang, L.; Kruse, B. *J. Opt. Soc. Am. A* **2004**, *21*, 1933. (d) Reyes-Coronado, D.; Rodriguez-Gattorno, G.; Espinosa-Pesqueira, M. E.; Cab, C.; de Coss, R.; Oskam, G. *Nanotechnology* **2008**, *19*, 145605.

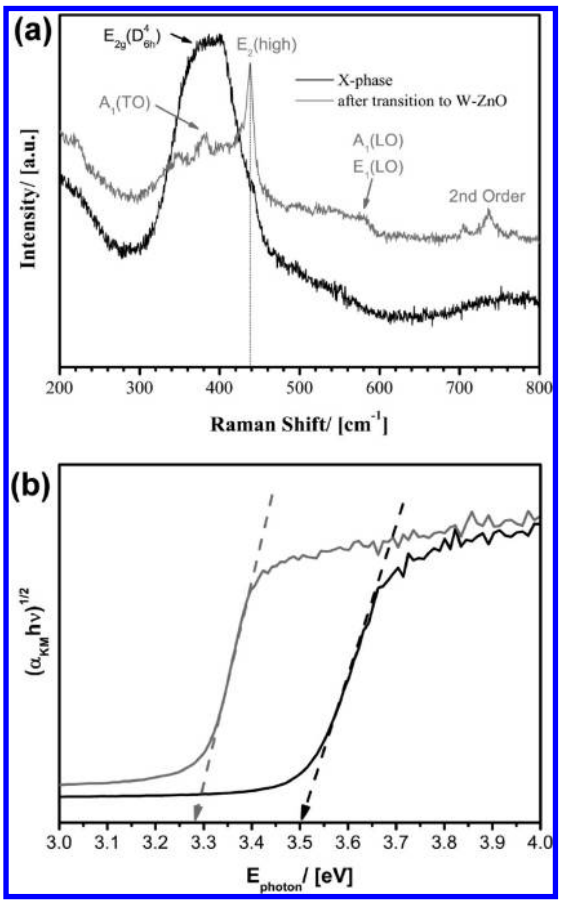

Figure 5. (a) Raman spectra of the X-phase (black) before and after the phase transition to W-ZnO (gray). (b) UV−vis spectra of the "X-phase" (black) and W-ZnO as a reference (gray) recorded in diffuse reflectance modus.

Conclusion

The conversion of a special organometallic zinc oxide precursor under kinetically controlled conditions resulted in a new product. The detailed analysis of this product with a variety of analytical methods including PXRD, DSC, XANES/EXAFS, HRTEM, FT-Raman and optical spectroscopy consistently point in the same direction: The new product is a metastable polymorph of zinc oxide with a structure resembling α-boron nitride (αBN-ZnO). The latter conclusion is also in accordance with theoretical studies that have reported the viability of αBN-ZnO.[18] The metastable phase transforms into Wurtzite at $T = 200$ °C. It is shown in Figure 2b that only a minor change in position of Zn^{2+} and O^{2-} along the crystallographic *c*-axis is necessary to result in W-ZnO.

However, different to our initial expectation discussed in relation to Scheme 1, the Rock Salt modification could not be prepared yet. This raises the question if the only function of the heterocubane precursor "Zn_4O_4" is to enable the rapid formation of ZnO at low temperatures or more. It was pointed out previously that the first step in the condensation reaction is the reaction of two heterocubanes to a molecular, octameric compound "Zn_8O_8" (see also Supporting Information, Figure SI-6).[30] Because the latter compound is a reactive intermediate, it was yet not possible to isolate it. Interestingly, Steudel and co-workers have predicted by ab initio calculations a "Zn_8O_8" cluster possesses a structure topologically directly correlated to the αBN-ZnO (Scheme 2b).[33] Bromley and co-workers have calculated similar nanocluster compounds as building blocks for ZnO.[34] Furthermore, Steiner and co-workers have published an experimental report about the transformation of two condensed heterocubanes to a hexaprismane structure for tris(organozinc) phosphazenates.[35] Therefore, it is likely that the described, labile intermediate also possesses the hexaprismane structure and reacts further to the αBN-ZnO structure (see Scheme 2). Thus, the work presented here represents a nice example for the application of Ostwald's step rule for the synthesis of metastable polymorphs.[36]

Experimental Section

Sample Preparation. All starting compounds were received from Sigma-Aldrich, and were purified and carefully dried prior to use. All reactions were performed under strict exclusion of air and humidity using Schlenk technique.

Preparation of $ZnMe_2$. $ZnCl_2$ is dried via the treatment with $SOCl_2$ under reflux. The remaining $SOCl_2$ is removed in vacuum. A solution of CH_3MgI (1.25 mol) in *n*-Bu_2O is slowly added to the $ZnCl_2$ (0.57 mol) under vigorous stirring. The suspension is heated for 60 h at 60 °C under reflux. The $ZnMe_2$ (bp = 43 °C) is collected by distillation in the temperature range of 130−160 °C; 40.8 g $ZnMe_2$ is obtained in 75% yield.

Preparation of the Precursor $[MeZnO^tBu]_4$. $ZnMe_2$ is diluted with freshly dried and distilled toluene. The solution is cooled to −78 °C. An equimolar amount of *tert*-butanol in toluene is added dropwise. The solution is warmed to room temperature and stirred for 12 h. The toluene is removed in vacuum. The resulting white solid is taken up in dry hexane. Residual solid products are separated by Schlenk centrifugation. The pentane is removed from the solution by vacuum drying.

Preparation of the X-Phase. A solution $[MeZnO^tBu]_4$ (c = 0.02 M) in a 1:1 mixture of tetrahydrofuran (THF) and CH_2Cl_2 is prepared. PVP ($M_w \approx 10$ KDa; 0.425 g) is added, followed by the addition of an equimolar amount of distilled water (relative to $[MeZnO^tBu]_4$) . The solution is kept stirring for 25 min at 25 °C. The solvents are rapidly removed from solution under vacuum. Finally, a mixture of distilled water (15 mL) and PVP (different ratios from 0 to 0.8 g PVP) is added. The temperature is carefully controlled during the addition. For obtaining the final product, the final solution is dried overnight.

Analytical Methods. X-ray diffraction was performed on a Huber G670 Guinier camera diffractometer using Cu $K\alpha_1$ radiation; the in situ X-ray diffraction measurements with temperature dependence were performed on a Bruker AXS D8 Advance diffractometer using Cu $K\alpha_1$ radiation and a Bruker AXS Sol-X solid state energy dispersive detector. DSC measurements were performed on a Netzsch DSC 204 F1 Phoenix, HRTEM measurements were performed by JEOL on a JEM-2100 microscope. XAS experiments were performed at beamline E4 (HASYLAB) at the Zn K-edge. The UV/vis measurements were done on a Varian Cary 100 scan UV/vis spectrophotometer. The Raman spectra were recorded with a LabRAM HR800 spectrometer (Horiba-Jobin-Yvon) using the 532.2 nm excitation

(33) Steudel, R.; Steudel, Y. *J. Phys. Chem. A* **2006**, *110*, 8912–8924.
(34) Carrasco, J.; Illas, F.; Bromley, S. T. *Phys. Rev. Lett.* **2007**, *99*, 235502.
(35) Boomishankar, R.; Richards, P. I.; Steiner, A. *Angew. Chem., Int. Ed.* **2006**, *45*, 4632.
(36) van Santen, R. A. *J. Phys. Chem.* **1984**, *88*, 5768.

line from a diode laser. The LabRAM integrated system was coupled through an Olympus MPlanN 50× objective (NA = 0.75) to the optical microscope. The spectra were collected in the backscattering geometry with a resolution of 2 cm^{-1}. The spectrally dispersed Raman signal was detected with a peltier-cooled CCD camera. The laser power on the sample was tuned to 1 mW.

Acknowledgment. We thank the Grillo Zinkoxid GmbH and The Deutsche Forschungsgemeinschaft (project PO780/4-1) for financial support. We thank JEOL and in particular Dr. M. Rodewald and O. Senftleben for their help with HRTEM and Dr. M. Krumova for electron diffraction measurements.

Supporting Information Available: Figure SI-1: alternative representation of the temperature-dependent PXRD data. Figure SI-2: Preparation of the X-Phase using an alternative agent for the colloidal stabilization of the growing ZnO particles, Palimitic acid. Figure SI-3: FT-IR and PXRD data of the as prepared X-phase containing PVP with pure PVP as a reference. Figure SI-4: Alternative representation of the ZnO phase with α-BN structure. Figure SI-5: Simulated X-ray absorption fine structure data, recorded at room temperature. Figure SI-6: Proposed mechanism for the formation of the reactive intermediate. This material is available free of charge via the Internet at http://pubs.acs.org.